PALEOBIOLOGY | Paleontological
A PUBLICATION OF THE | SOCIETY

Benthic community history in the Changjiang (Yangtze River) mega-delta: Damming, urbanization, and environmental control

Richard Ching Wa Cheung ⓘ, *Moriaki Yasuhara, Hokuto Iwatani, Chih-Lin Wei, and Yun-wei Dong*

Abstract.—The coastal environment of the Changjiang delta has been influenced by recent anthropogenic activities such as dam construction and increased sewage and fertilizer inputs. Previous work examined the compositional shift of marine plankton to assess ecological impacts of these activities on marine ecosystems in the Changjiang discharge area. Here we used benthic marine ostracodes collected in the Changjiang estuary and the adjacent East China Sea in the 1980s and the 2010s, respectively, to investigate temporal changes of the benthic community and controlling factors for the benthic fauna. Our results revealed more shoreward distribution of some well-known offshore ostracode species in the 2010s compared with the 1980s and a relatively more important role for environmental processes (e.g., bottom-water temperature, bottom-water salinity, and eutrophic conditions of surface water) than spatial processes (e.g., the flow of ocean currents) in structuring ostracode compositions. The temporal changes in the ostracode community are likely attributable to the combined effects of reduced fresh water and sediment discharge and eutrophic conditions of the Changjiang due to the many dams constructed along the Changjiang and population expansion in the Changjiang Basin. Results of redundancy analysis and variation partitioning suggest that ocean currents facilitated environmental filtering of ostracode species such that they could disperse to preferred environmental conditions. These findings highlight the potential uses of marine microfossils to better understand ecological impacts on benthic ecosystems in vulnerable Asian mega-deltas and provide insights into the integration of metacommunity concepts in disentangling dynamics of marine benthic communities.

Richard Ching Wa Cheung, Moriaki Yasuhara, and Hokuto Iwatani. School of Biological Sciences and Swire Institute of Marine Science, University of Hong Kong, Kadoorie Biological Sciences Building, Pokfulam Road, Hong Kong SAR, China. E-mail: h1026139@connect.hku.hk, moriakiyasuhara@gmail.com, hokuto.iwatani@gmail.com

Chih-Lin Wei. Institute of Oceanography, National Taiwan University, No.1, Section 4, Roosevelt Road, Taipei 106, Taiwan.

Yun-wei Dong. State Key Laboratory of Marine Environmental Science, College of Ocean and Earth Sciences, Xiamen University, Xiamen, China.

Introduction

Large rivers carry freshwater and land-derived materials to the ocean (Meybeck and Vörösmarty 2005) and determine the physical and biogeochemical characteristics of estuaries and ocean margins (McKee et al. 2004; Meybeck et al. 2006; Bianchi and Allison 2009). Deltas are formed when a considerable amount of sediment is deposited at rates faster than it can be redistributed by marine processes (Woodroffe and Saito 2011). However, many deltas of the world have been shrinking, mostly owing to human activities such as groundwater extraction and dam constructions (Syvitski et al. 2009). In particular, among large-river deltas, the Asian mega-deltas are now

considered to be the most vulnerable to anthropogenic impacts (Saito et al. 2007).

The Changjiang (Yangtze River) delta is characterized by discharge of the Changjiang, which is the longest river in China and a major source of terrestrial sediments in the East China Sea (ECS) (Bianchi and Allison 2009; Gu et al. 2011). Over the past decades, anthropogenic activities have altered sediment flux and water discharge of the Changjiang. Soil-conservation projects in the Changjiang Basin reduced sediment flux at Datong (a downstream water-monitoring station) by ca. 3 Mt/yr (Yang et al. 2015). In addition, both the number and the scale of dams in the Changjiang Basin increased significantly from the

1980s to the 2010s, with nearly 200 large dams in existence in 2015 (Yang et al. 2018), and these dams have led to coastal erosion in the delta by reducing sediment deposition levels (Saito et al. 2007; Wang et al. 2011; Yang et al. 2018). The Three Gorges Dam (TGD), the largest dam in the world (Nilsson et al. 2005), is located in the middle reach of the Changjiang (Guo et al. 2012). Since the TGD began operating in 2003, it has played an influential role in accounting for decreased mean annual water discharge and mean sediment flux of the Changjiang (Yang et al. 2015, 2018). Changes in sedimentary processes were reported to result in temporary shrinking of the relatively high primary production area and shifting of phytoplankton species composition in the Changjiang diluted water zone (Gong et al. 2006). Populations and fertilizer use in the main provinces and cities (except Shanghai) in the Changjiang basin have been increasing (Chai et al. 2009). From 1970 to 2013, dissolved inorganic nitrogen and dissolved inorganic phosphate fluxes to the Changjiang estuary increased by 338% and 574%, respectively (Wang et al. 2015). Ecological impacts of the TGD on terrestrial and/or aquatic biodiversity were assessed in the TGD reservoir area, that is, the upper and middle Changjiang (Wu et al. 2004; Shao et al. 2008; Duan et al. 2009; Wang et al. 2010). Impacts of these anthropogenic impacts on the benthic marine ecosystem in the Changjiang estuary and its adjacent sea, however, remain poorly understood.

Ostracoda are a group of tiny bivalved crustaceans that distribute ubiquitously in shallow-marine habitats (Schellenberg 2007). The robust species-level taxonomy (Yasuhara et al. 2017) in addition to sensitivity to environmental changes (Athersuch et al. 1989; Boomer and Eisenhauer 2002) allows microfossil ostracodes to be a good model system to assess biogeography and environment–assemblage relationships in Asian mega-deltas. Furthermore, modern ostracodes in Changjiang estuary and its nearby shelf were investigated in the 1980s (Wang and Zhao 1985; Zhao 1987; Wang et al. 1988; Zhao and Wang 1988), providing a baseline to allow comparison of ostracode distribution before and after increased anthropogenic activities, including major dam constructions

in the Changjiang. However, understanding of environment–ostracode association in past studies was hindered by insufficient environmental data and statistical methods. Here, we examined (1) similarities of ostracode composition and species distribution between the 1980s and the 2010s, and (2) the species–environment relationship of modern ostracode faunal compositions in the Changjiang estuary and its nearby marine area.

Material and Methods

Study Area and Ostracode Sampling.—Surface-grabbed samples (~100 ml) were collected by a modified Van Veen Grab in 2014 at 26 sites in Changjiang estuary and its nearby marine area (Fig. 1). The Changjiang diluted water (CDW) and the Taiwan Warm Current (TWC) are primary water sources that determine physicochemical properties of both surface and bottom water in this area (Chen et al. 2003). Their temperature and salinity levels exhibit seasonal variation (Table 1).The CDW forms when freshwater discharged from the Changjiang mixes with seawater, forming an area with low salinity and high nutrient content (Gong et al. 2006), which alters environmental parameters in the Changjiang estuary and its adjacent coastal waters (Lie et al. 2003; Liu et al. 2006; Kako et al. 2016). On the other hand, the TWC is a near-bottom ocean current that enters the study area along the 50 m isobath (Chen et al. 2003). Coastal and northern study sites are more affected by the CDW, while those located in the central and southern parts of the study area are more influenced by the TWC (Fig. 1). The sedimentation rate in our study region can reach up to 5 cm/yr (De Master et al. 1985). A more recent estimation by Su and Huh (2002) suggests that the sedimentation rate is approximately 1–2 g/cm/yr.

The sediments were washed through a 63 μm mesh sieve and then oven-dried at 40°C for 1 day. Then, we dry-sieved the residues with a 150 μm mesh sieve to pick ostracod specimens from >150 μm fractions. Ostracode-rich samples were divided into fractions containing around 100–200 valves using a sample splitter. For ostracode-poor samples, all specimens in a sample were picked. The total number of specimens
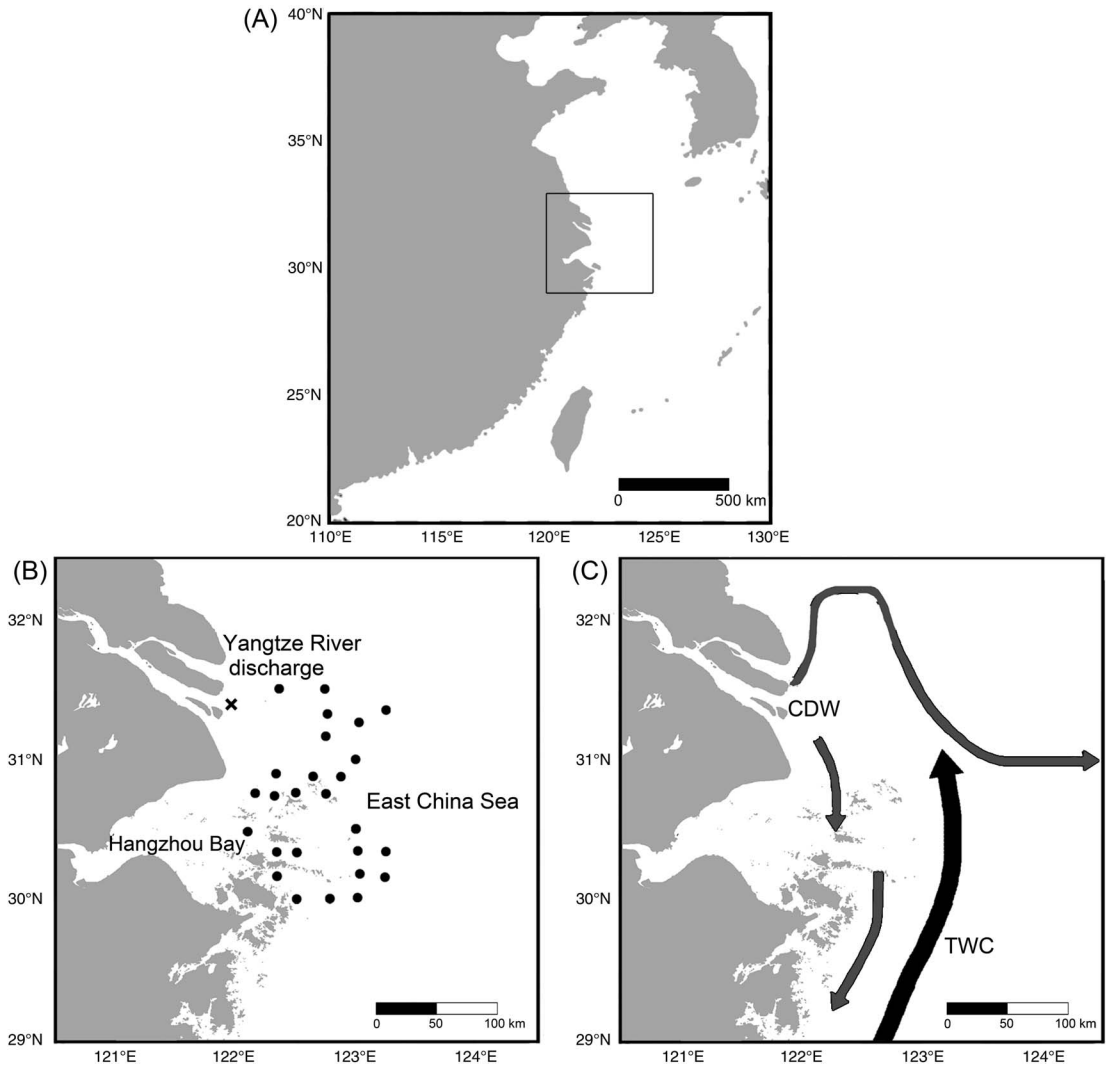
FIGURE 1. Maps showing locations of sampling sites of this study, and the regional ocean current flowing pattern. A, The square indicates the location of our study region in the East China Sea. B, The 26 sampling sites of this study are represented by black points. Point X (31.3937°N, 121.9485°E) represents the designated river mouth position, which was used as a referencing location to compare changes in species distribution between the 1980s and the 2010s. C, Directions of Changjiang diluted water (CDW) and Taiwan Warm Current (TWC) are indicated by arrows, respectively (after Chen et al. 2003).

TABLE 1. Physicochemical properties of the Changjiang discharge water (CDW) and the Taiwan Warm Current (TWC). Data are from Chen et al. (2009).

	Summer		Winter	
	Temperature, °C	Salinity, psu	Temperature, °C	Salinity, psu
CDW	27-29	20-31	6-17	<32
TWC	20-23	34-34.5	11-18	33-34.5

refs to the sum of left and right valves. One carapace was counted as two valves.

Sources of the Ostracode Data from the 1980s.—Grab and core-top sediment samples were collected during cruises organized by the Second Institute of Oceanography, China and Tongji University. Fifty grams of sediment from each sample was washed on 63 μm (or 55 μm) sieves;

more than 100 ostracode specimens were picked from each sample; and samples containing highly abundant ostracode specimens were split into smaller fractions (Zhao and Wang 1988). Percent (relative) abundance data for the ostracode species collected in the 1980s at sampling stations in Wang and Zhao (1985) and Wang et al. (1988) were obtained from two sources: (1) 28 sampling sites containing raw count data collected by Quanhong Zhao, who investigated ostracodes for Wang and Zhao (1985) and Wang et al. (1988); and (2) 9 sites for which raw census recording materials had been lost, so percent abundance information for ostracode species listed in Wang and Zhao (1985) and Wang et al. (1988) was used.

To examine temporal changes in the distributional pattern of some key species, percent abundance of these species at different sampling sites was plotted against the distance between the corresponding site and a designated river mouth position (point X; 31.3937° N, 121.9485°E; see Fig. 1). Synonyms of ostracode species occurring in both the studies from the 1980s and this study were identified mainly based on Hou and Gou (2007).

Source of Environmental Variables.—Bottom-water salinity was suggested to be the most important environmental factor governing ostracode composition in the study region of the present study (Zhao 1987), while combined effects of water depth and bottom-water temperature and salinity were significant at a larger spatial extent (Zhao and Wang 1988). However, shallow-marine ostracode compositions can also be significantly related to other variables, such as surface productivity (Yasuhara et al. 2012b) and grain size of substrates (Frenzel and Boomer 2005; Irizuki et al. 2006). Most of these environmental variables are known to exhibit seasonal variations in the Changjiang estuary and its adjacent sea (Pei et al. 2009; Kako et al. 2016). To assess their influences on ostracode distributions, we included (1) water depth, (2) mud content (dry weight percentage of <63 μm size fraction sediment of each sampling location), (3) seasonal bottom-water temperature and salinity data from the 2013 World Ocean Atlas (WOA) v. 2 (quarter-degree version; Locarnini et al. 2013; Zweng et al. 2013), and (4) monthly ocean surface-productivity

data represented by chlorophyll A readings from NASA's OceanColor Web (unit: mg/m^3; grid size: 0.1°; NASA Goddard Space Flight Center et al. 2014) in the statistical analyses. Following the data format of WOA 2013, the seasonal environmental data were classified into four periods: January–March, April–June, July–September, and October–December. Seasonally (instead of annually) averaged data were used, because both water and sediment discharges of the Changjiang apparently demonstrate seasonal variation, which is mainly dependent on the timing of retention and release of water stored in the TGD reservoir (Gao et al. 2013).

Statistical Analyses.—Ostracode faunal data at 26 sampling sites from the present study and 22 sites from the 1980s studies were combined. Similarities of ostracode composition at these 48 locations were investigated by cluster analysis and nonmetric multidimensional scaling (NMDS). *Bicornucythere bisanensis* forma P and forma G of Abe (1988) were combined as *Bicornucythere bisanensis* sensu lato to match with the taxonomic identification of the data from the 1980s. Percent abundance of ostracode species was first square-root transformed (i.e., Hellinger transformed; Legendre and Gallagher 2001) before calculation of the Euclidean dissimilarity matrix. The unweighted pair group method with arithmetic mean (UPGMA) was used as a clustering method. A Kelley-Gardner-Sutcliffe (KGS) penalty function (Kelley et al. 1996), which maximized the differences between the groups and the cohesiveness within groups, was computed to determine the optimal number of cluster groups. NMDS was performed using the same dissimilarity matrix to visualize the pattern of cluster groups. Ostracod species diversity was calculated as rarefaction ([E(S$_{50}$)], estimated number of species when the sample size was 50) to address sample size artifact.

Twenty-one samples collected in this study comprising more than 100 specimens were considered in examining environment–species association. Sixty ostracode species with three or more specimens in any one sample were included in the redundancy analysis (RDA) models. *Bicornucythere bisanensis* forma P and forma G of Abe (1988) were considered as

two species in the RDA. Species composition data sets were first normalized by log $(x + 1)$ transformation, then Hellinger transformed (Legendre and Gallagher 2001) before calculation of the Euclidian dissimilarity matrices.

Environmental variables were normalized by log transformation. Their collinearity was examined by computing variance inflation factors (VIF). A VIF greater than 10 indicated significant collinearity (O'Brien 2007). RDA was then carried out to identify the relationship between ostracode composition and environmental variables. Water depth was one of the factors that showed high VIF and thus was excluded in the RDA. The adjusted R^2 values for RDA models before and after removing water depth as an explanatory variable were similar. Forward selection with two stopping criteria (Blanchet et al. 2008) was applied to select significant ($p < 0.05$) environmental predictors in the RDA model (hereafter referred as Spe-Env RDA) by permutation tests using 9999 randomizations.

Spatial predictors were generated by means of distance-based Moran's eigenvector maps (dbMEM) (Dray et al. 2006), using the largest distance in the minimum spanning tree connecting all sites as the truncation distance. A set of orthogonal spatial predictors containing dbMEM eigenvectors was produced. Positive (negative) eigenvalues of the dbMEM variables represent positive (negative) spatial processes, corresponding to broadscale (fine-scale) spatial patterns (Dray et al. 2012). Only dbMEM variables with significant Moran's I values were considered in further analysis. Geographical coordinates of sampling units were also included as spatial predictors, because dbMEM variables were insufficient to cover linear trends of spatial processes (Buschke et al. 2015). Forward selection of the spatial variables was then conducted. RDA was performed using species data as the response variables and spatial variables as the explanatory variables (hereafter referred as Spe-Spa RDA).

Variation partitioning was finally conducted on the environmental and spatial variables described to determine unique and combined contributions of environmental and spatial processes in explaining variation of ostracode composition (Borcard et al. 1992; Peres-Neto et al. 2006; Peres-Neto and Legendre 2010). Eventually, the variation was partitioned into fractions based on (1) pure environmental processes, (2) pure spatial processes, (3) spatially structured environmental factors, and (4) unexplained variance. We report the unbiased amount of explained variation (adjusted R^2) by correcting R^2 values, which was suggested to be a better estimator of the population values, following the procedures outlined in Peres-Neto et al. (2006).

All analyses were conducted in R programming language (R Core Team 2017), using the packages 'ggmap' (Kahle and Wickham 2013), 'ggplot2' (Wickham 2016), and 'ggsn' (Baquero 2017) for mapping; 'stats' (R Core Team 2017) and 'maptree' (White and Gramacy 2012) for cluster analysis; 'adespatial' (Dray et al. 2017) for dbMEM, 'packfor' (Dray et al. 2013) for forward selection; 'iNEXT' (Hsieh et al. 2016) for estimation of rarefied species richness; and 'vegan' (Oksanen et al. 2017) for cluster analysis, RDA, and variance partition.

Results

The KGS penalty function suggested three clusters as the optimal number of groups (Supplementary Fig. S1). Generally, the overall ostracode community displayed three major groups from the coast to the sea (Fig. 2): estuary (ES; $n = 16$), inner shore (IS; $n = 23$), and offshore (OS; $n = 9$). Ostracode species diversities were generally similar between the 1980s and 2010s (Fig. 3). Changes of ostracode species distribution relative to the studies from the 1980s were characterized by the following patterns (Figs. 4–6): (1) increased percent abundance in the inner-shore region: *Cytheropteron subuchioi* (Fig. 4A), *Neosinocythere elongata* (Fig. 4B), and *Nipponocythere bicarinata* (Fig. 4C); (2) more widespread distribution in the whole region: *Pistocythereis bradyformis* (Fig. 5C); (3) reduced percent abundance in the inner-shore region of the study area: *Cytheropteron miurense* sensu lato (Fig. 6A), *Munseyella japonica* (Fig. 6B), *Stigmatocythere roesmani* (Fig. 6C). Taxonomic synonyms of the above-named species identified in Wang et al. (1988) are listed in Table 2.

Effects of environmental variables on species composition of 60 ostracode species were tested
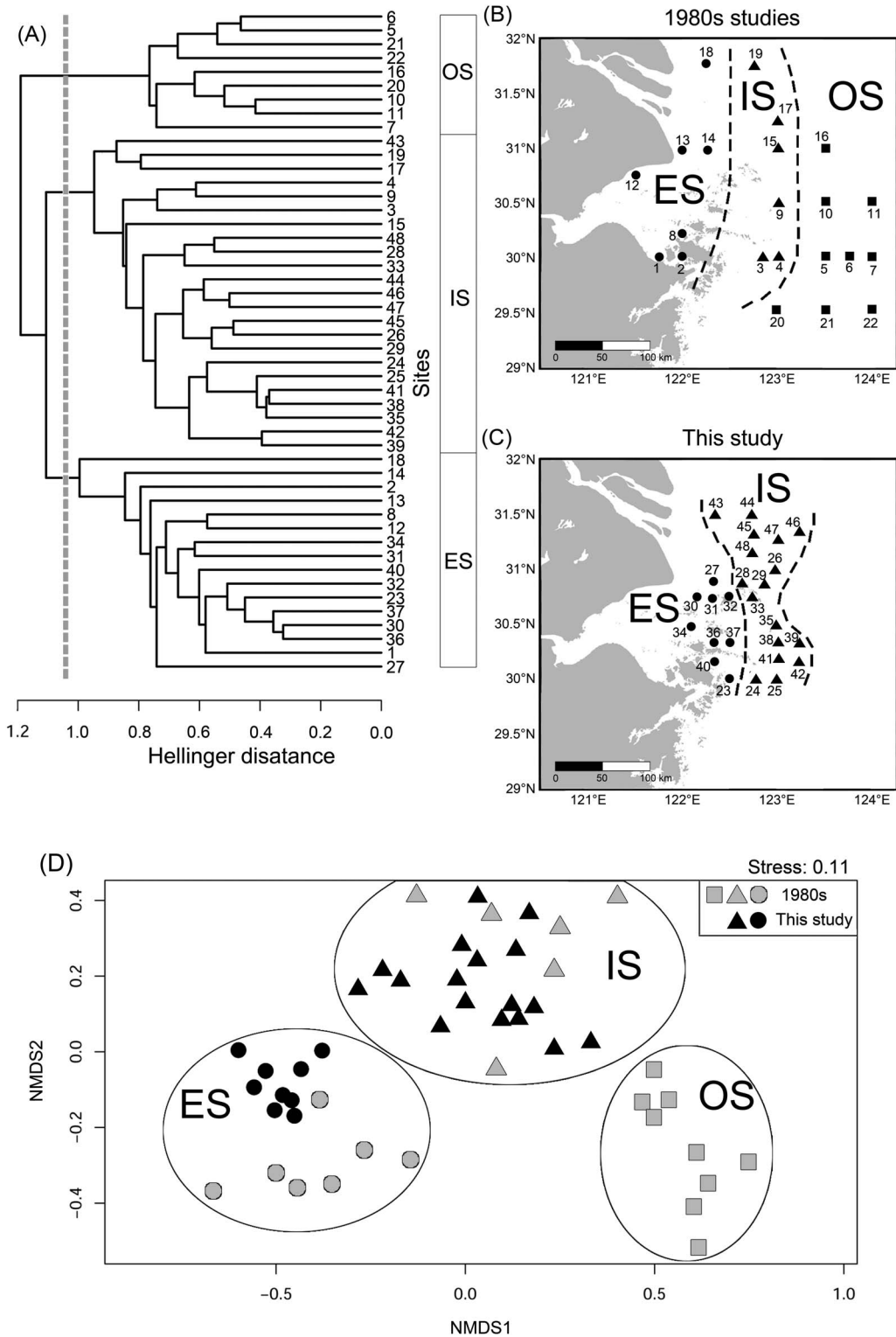
FIGURE 2. Combined analysis of relative abundance of ostracode species. A, Unweighted pair group method with arithmetic mean clustering results. OS (offshore), IS (inner shore), and ES (estuary) denote ostracode biofacies. B, Map showing distribution of sampling sites in Wang and Zhao (1985) and Wang et al. (1988). C, Map showing distribution of sampling sites in this study. Numbers refer to the site described in Supplementary Table S2. D, Nonmetric multidimensional scaling (NMDS) plot visualizing similarities of ostracode composition at different sites. OS, squares; IS, triangles; ES, circles.
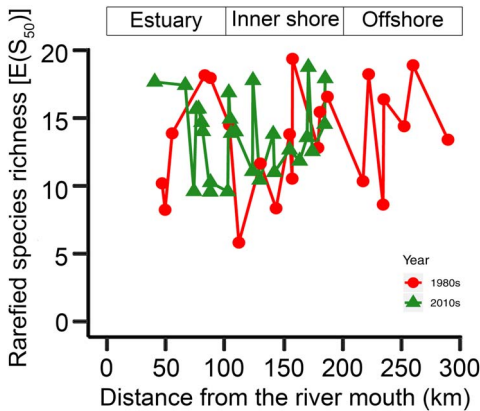
FIGURE 3. Comparison of rarefied species richness [E(S$_{50}$)] of ostracode community in the Changjiang estuary and the adjacent East China Sea in the 1980s (gray dashed line) and the 2010s (black solid line). Sampling sites in the 1980s (Wang and Zhao 1985; Wang et al. 1988) and the 2010s (this study) are denoted by dots and triangles, respectively. The x-axis is the distance from the river mouth ("X" in Fig. 1; see "Materials and Methods" section).
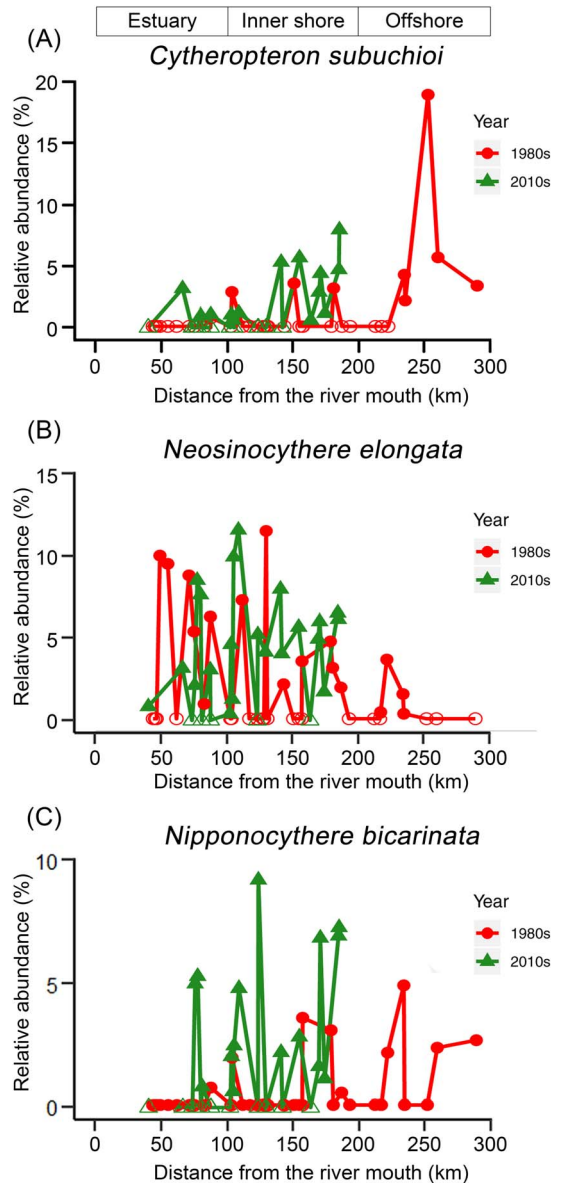

FIGURE 4. Comparison of percent (relative) abundance of ostracode species. A, *Cytheropteron subuchioi*; B, *Neosinocythere elongata*; and C, *Nipponocythere bicarinata*, in the Changjiang estuary and the adjacent East China Sea in the 1980s (circles) vs. the 2010s (triangles). For sampling sites containing less than 1% of the corresponding species in Wang and Zhao (1985) and Wang et al. (1988), percent abundance of that corresponding species was truncated to 0.1%. Zero abundance is represented by open circles/triangles. The x-axis is the distance from the river mouth ("X" in Fig. 1; see "Materials and Methods" section).

in RDA. Forward selection of environmental variables retained four significant factors ($p <$ 0.05) for further analysis, namely, bottom-water salinity in January–March and July–September, bottom-water temperature in July–September, and surface productivity in October–December. They jointly accounted for 44.3% (adjusted R^2; $p = 0.001$) of the variation in the species composition (Table 3). July–September temperature (adjusted $R^2 = 0.159$; $p < 0.001$) and salinity (adjusted $R^2 = 0.141$; $p = 0.001$) together represent ~68% of the explained variance.

Forward selection on the spatial variables resulted in four significant spatial predictors (MEM1, MEM 2, MEM 4, and MEM 7; Supplementary Fig. S7). The spatial model significantly accounted for 41.1% (adjusted R^2; $p = 0.001$) of the variation of ostracode composition (Table 3).

An RDA plot (Fig. 7, Table 4) showed that *Bicornucythere bisanensis* (forma P of Abe 1988) was negatively related to July–September bottom-water salinity. Its unique position in the lower right quadrant indicated a distinct ecological niche for this species compared with other species in this study. *Cytheropteron subuchioi*, *Cytheropteron miurense* sensu lato, *Munseyella japonica*, *Cytherelloidea yingliensis* sensu lato, and *Bicornucythere bisanensis* (forma G of Abe 1988) showed a positive

relationship with the July–September salinity. *Albileberis sinensis* was more positively associated with higher July–September bottom-
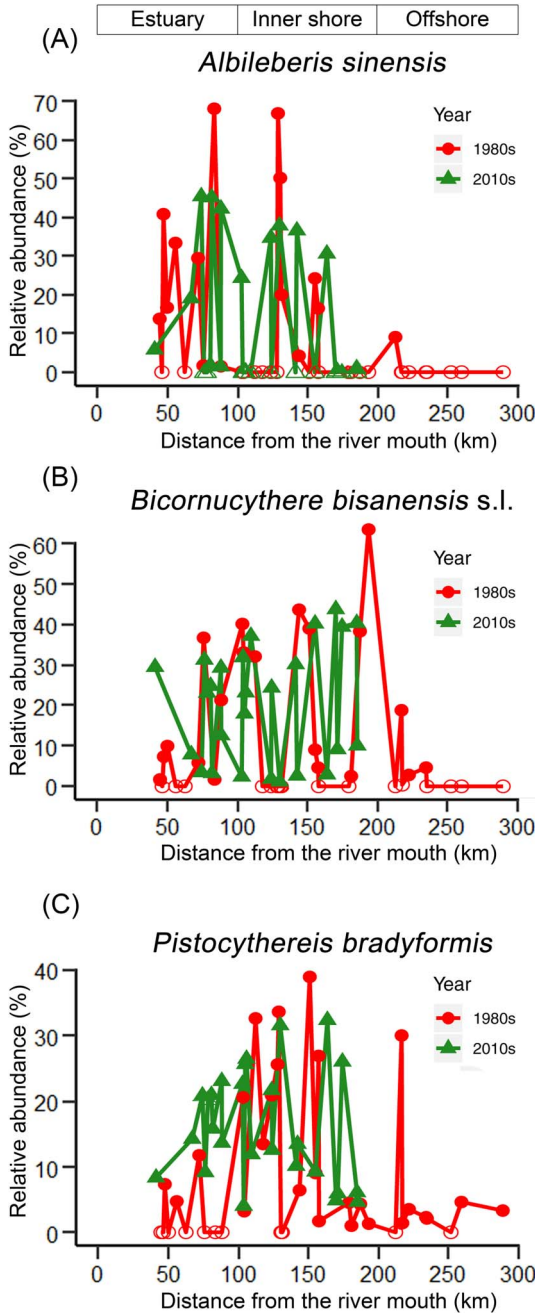
FIGURE 5. Comparison of percent (relative) abundance of three most abundant ostracode species. A, *Albileberis sinensis*; B, *Bicornucythere bisanensis* sensu lato; and C, *Pistocythereis bradyformis* in the Changjiang estuary and the adjacent East China Sea in the 1980s (circles) vs. the 2010s (triangles). For sampling sites containing less than 1% of the corresponding species in Wang and Zhao (1985) and Wang et al. (1988), percent abundance of that corresponding species was truncated to 0.1%. Zero abundance is represented by open circles/triangles. The x-axis is the distance from the river mouth ("X" in Fig. 1; see "Materials and Methods" section).
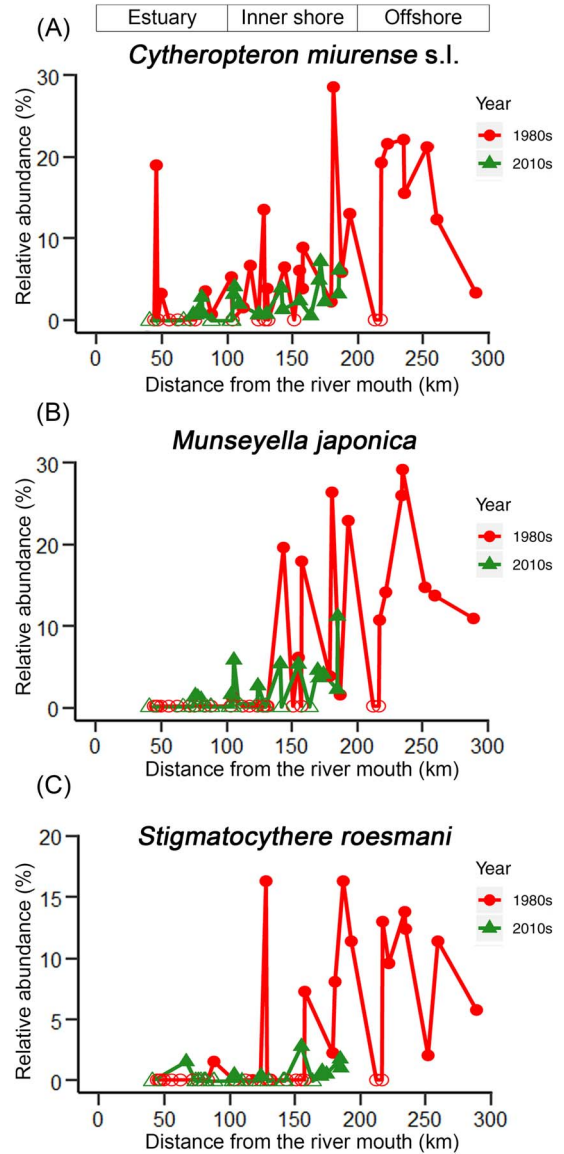

FIGURE 6. Comparison of percent (relative) abundance of ostracode species. A, *Cytheropteron miurense* s.l.; B, *Munseyella japonica*; and C, *Stigmatocythere roesmani* in the Changjiang estuary and its adjacent East China Sea in the 1980s (circles) vs. the 2010s (triangles). For sampling sites containing less than 1% of the corresponding species in Wang and Zhao (1985) and Wang et al. (1988), percent abundance of that corresponding species was truncated to 0.1%. Zero abundance is represented by open circles/triangles. Zero abundance is represented by open circles/triangles. The x-axis is the distance from the river mouth ("X" in Fig. 1; see "Materials and Methods" section).

water temperature and lower bottom-water salinity, whereas *Nipponocythere bicarinata*, *Neosinocythere elongata*, and *Bicornucythere*

TABLE 2. Taxonomic synonyms for ostracode species in this study and the studies from the 1980s.

Ostracode species in this study	Synonymized species in Wang et al. (1988)
Alocopocythere kendengensis	*Alocopocythere profusa*
Bicornucythere bisanensis s.l. (i.e., forma P and G of Abe 1988)	*Bicornucythere bisanensis*
Cytherelloidea yingliensis s.l.	Specimens in the current study are morphologically similar to *Cytherelloidea yingliensis* (Wang et al. 1988: Plate XXXV, nos. 11,12). Posteroventral ridge of the former is straight, while that of the latter is curved.
Cytheropteron donghaiensis	*Kobayashiina donghaiensis*
Cytheropteron miurense s.l.	Specimens in the current study are morphologically similar to *Cytheropteron miurense* (Wang et al. 1988; Plate LII, nos. 10,11). The former lacks a posterodorsal node.
Keijella apta	*Cathetocytheretta apta*
Leptocythere ventriclivosa s.l.	Specimens in the current study are morphologically similar to *Leptocythere ventriclivosa* (Wang et al. 1988: Plate XXXVIII, nos. 13,14). Valves of the former are ornamented, while those of the latter are smooth.
Neomonoceratina dongtaiensis	*Neomonoceratina crispata*
Neosinocythere elongata	*Sinocythere? reticulata*
Pistocythereis bradyformis	*Echinocythereis? bradyformis*
Sinocytheridea impressa	*Sinocytheridea latiovata*
Stigmatocythere roesmani	*Stigmatocythere spinosa*
Trachyleberis niitsumai s.l.	*Acanthocythereis niitsumai*
Trachyleberis scabrocuneata s.l.	*Trachyleberis scabrocuneata*

bisanensis (forma G of Abe 1988) were associated with lower July–September bottom-water temperature. Distributions of *Trachyleberis niitsumai* sensu lato, *Keijella apta*, *Hanaiborchella miurensis*, and *Cytheromorpha acupunctata* were more dependent on lower January–March bottom-water salinity.

The whole model of variation partition analysis accounted for 47.3% of the variation of ostracode composition (Fig. 8). The largest explained fraction was attributed to the joint effect of environmental processes and spatial processes fraction [b] (adjusted $R^2 = 0.38$). A significant pure environmental fraction [a] (adjusted $R^2 = 0.063$; $p = 0.001$) and an insignificant pure spatial fraction [c] (adjusted $R^2 = 0.03$; $p = 0.103$) were identified (Table 1).

TABLE 3. Results of the redundancy analysis (RDA) variation partitioning of ostracode community. Spe-Env RDA, environmental predictors in the redundancy analysis model; Spe-Spa RDA, spatial predictors in the redundancy analysis model; MEM, Moran's eigenvector maps; fraction [a] represents pure environmental processes; fraction [c] represents pure spatial processes; fraction [b] represents the shared effect of the two processes; an asterisk (*) indicates significance of the shared fraction is not testable.

	Adjusted R^2, %	p	Selected variables
Spe-Env	44.3	0.001	July – Sept temperature, July – Sept salinity, Jan – Mar salinity, and Oct – Dec surface productivity
Spe-Spa	41.1	0.001	MEM 1, MEM 2, MEM 4, and MEM 7
[a]	6.3	0.001	
[c]	3.0	0.103	
[b]*	38.0		

TABLE 4. Ostracode species and their codes used in redundancy analysis models.

Species	Code
Albileberis sinensis	AS
Alocopocythere kendengensis	AlK
Bicornucythere bisanensis (forma G of Abe 1988)	BG
Bicornucythere bisanensis (forma P of Abe 1988)	BP
Keijella apta	CP
Cytherelloidea yingliensis s.l.	CY
Cytheromorpha acupunctata	CyA
Cytheropteron donghaiense	CD
Cytheropteron miurense s.l.	CMi
Cytheropteron subuchioi	CSu
Leptocythere ventriclivosa s.l.	LV
Loxoconcha ocellata	LO
Munseyella japonica	MJ
Munseyella pupilla	MP
Neomonoceratina dongtaiensis	NDo
Neosinocythere elongata	NE
Nipponocythere bicarinata	NB
Hanaiborchella miurensis	PM
Pistocythereis bradyformis	PB
Sinocytheridea impressa	SI
Stigmatocythere roesmani	SR
Tanella opima	TO
Trachyleberis niitsumai s.l.	TN
Trachyleberis scabrocuneata s.l.	TslS

Discussion

Comparing Similarities of Ostracode Compositions in the 1980s and the 2010s.—The high sedimentation rate in the study area suggests that ostracode valves collected in this study likely represent the fauna of the 2010s and considerable mixing with older (e.g., 1980s) ostracode valves is unlikely. Moreover, dominant species in our study such as *Pistocythereis bradyformis*, *Bicornucythere bisanensis*, *Nipponocythere bicarinata*, and *Sinocytheridea impressa* were abundantly found in muddy sediments (Fujiwara et al. 2000; Irizuki et al. 2006; Hong et al. 2019). High abundance of these species in our samples indicates a low-energy environment and autochthonous fauna at the sites studied. Clustering results and the NMDS ordination broadly divide ostracode communities into three major groups corresponding to their distances from the coast (Fig. 2). For example, the ES biofacies is comprised of the ostracode assemblage of inner Hanzhou Bay from the 1980s (Fig. 2B) and the coastal assemblage from the 2010s (Fig. 2C). These two assemblages share the same dominant species (i.e., *Albileberis sinensis*; Fig. 5A). The IS biofacies appears to be found along 123°E in both the 1980s and the 2010s. This is likely due to the dominance of *Bicornucythere bisanensis* (Fig. 5B) and *Pistocythereis bradyformis* (Fig. 5C) over the past decades. On the other hand, the OS biofacies, which is dominated by *Cytheropteron miurense* sensu lato (Fig. 6A), *Stigmatocythere roesmani* (Fig. 6B), and *Munseyella japonica* (Fig. 6C) does not have a counterpart in the 2010s.

Impacts of Dams and Anthropogenic Inputs on Ostracode Distribution over the Past 30 Years.—Ostracode species such as *Cytheropteron subuchioi* (Fig. 4A), *Neosinocythere elongata* (Fig. 4B), and *Nipponocythere bicarinata* (Fig. 4C) that are known to inhabit relatively offshore, oceanic areas in the China seas and Japanese bays (Zhao and Wang 1988; Yasuhara et al. 2005; Yasuhara and Seto 2006; Chunlian et al. 2013) show more landward distribution in the 2010s. The RDA results indicate that these species are more related to saline summer bottom water (Fig. 7). Given that more shoreward intrusion

of saline water into the inner-shore area of the Changjiang discharge area has been reported as a consequence of lower summer water discharge of the Changjiang after construction of the TGD (Gong et al. 2006; Jiao et al. 2007; Chen et al. 2009; Tsai et al. 2010), the distributional changes of these species likely represent a response to this dam-induced reduction of river water discharge.

Relative abundance of species such as *Albileberis sinensis* (Fig. 5A), *Bicornucythere bisanensis* (Fig. 5B), and *Pistocythereis bradyformis* (Fig. 5C) also increased in the Changjiang discharge area from the 1980s to the 2010s. However, the RDA plot indicates that the driving factors for the distributional changes of these species could be complicated. For example, occurrences of *Albileberis sinensis* and *Cytheromorpha acupunctata* are more related to warmer July–September water temperature and higher October–December surface productivity, respectively (Fig. 7), suggesting the potential contribution of hydrological parameters in various seasons. Apart from this, the higher percent abundance of *Bicornucythere bisanensis*, which is a well-known eutrophication-resistant species (Yasuhara et al. 2007, 2012a; Irizuki et al. 2011) showing strong positive correlation with total organic carbon content in Kasado Bay, Japan (Irizuki et al. 2015), may be attributed to increased organic matter as a result of escalated fertilizer use and sewage discharge in the Changjiang Basin since the 1990s (Chai et al. 2009).

Controlling Factors of Ostracode Species Compositions.—Among the environmental factors included in this study (measured during 2005 to 2012), bottom-water temperature and salinity in July–September most significantly explain variation of ostracode composition. Shallow-marine ostracode faunal characteristics and distributions have been related to bottom temperature and/or salinity (Bodergat and Ikeya 1988; Ozawa et al. 2004; Yasuhara et al. 2012b), in particular, some species may respond to seasonal variation of environmental variables (Brouwers et al. 2000). The greater importance of environmental variables in July–September may be related to ostracode species tolerance limits with respect to the summer environment, that is, maximum temperature and/or minimum salinity, which
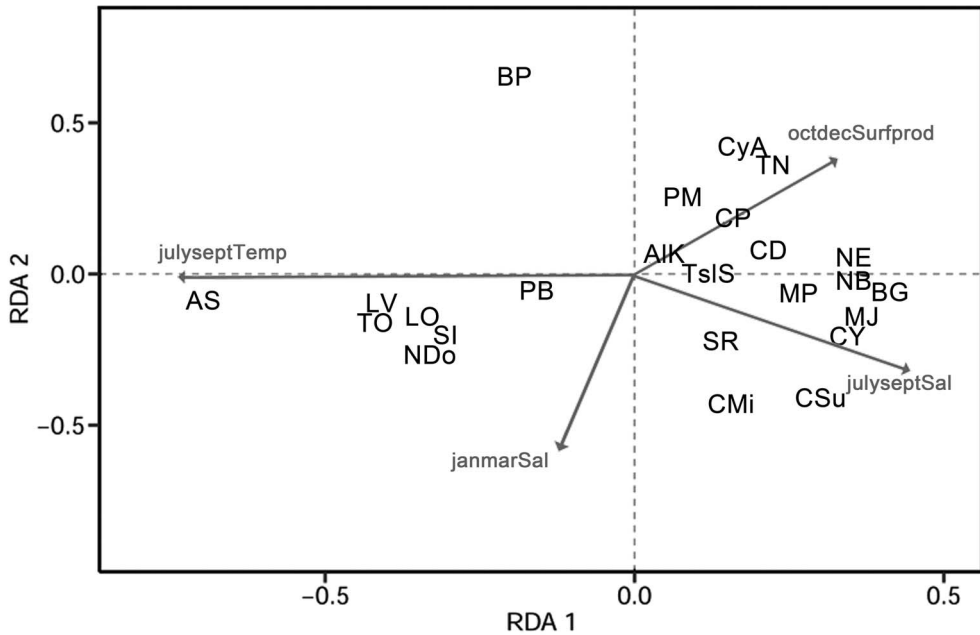
FIGURE 7. Environmental predictors in the redundancy analysis model (Spe-Env RDA) biplots for ostracode compositions. Significant environmental variables are shown. Projecting species objects at right angles on an environmental variable approximates their positions along that variable. Cosine of an angle between response and explanatory variables represents their correlation. janmarSal, bottom-water salinity in January–March period; julyseptSal, bottom-water salinity in July–September; julyseptTemp, bottom-water temperature in July–September; octdecSurfprod, surface productivity in October–December. For species abbreviations, see Table 2.

can potentially be regulated by variability of the TWC strength (a branch of Kuroshio Current), climate variables (e.g., monsoon precipitation), and water discharge patterns of the Changjiang.

A large proportion of the variation in ostracode composition is explained by the fraction
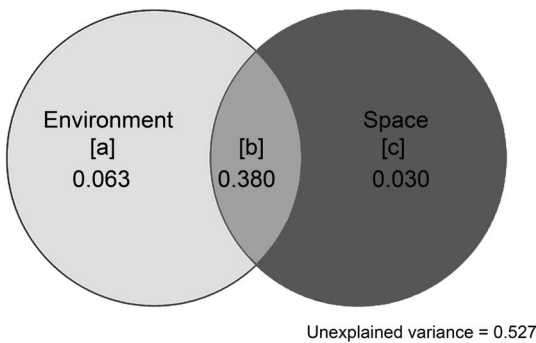

FIGURE 8. Venn diagram showing results of variation partitioning: [a] is pure environmental fractions, [b] is joint fractions shared by environmental and spatial processes, and [c] is pure spatial fractions. Adjusted R^2 values are reported.

of spatially structured environmental variables (fraction [b]; Fig. 8). This fraction could either be attributed to spatially structured environmental variables (i.e., bottom-water temperature and salinity) or to spatial variation of some unobserved environmental factors that affected both the ostracode community structure and the explanatory variables in the analysis (Legendre and Legendre 2012). Adjusted R^2 values of the purely environmental component [a] and purely spatial component [c] are relatively low, yet they are consistent with the results of De Bie et al. (2012), who reported the explained variation by other passively dispersed aquatic organisms driven by [a] and [c].

Dispersal is an important mechanism in community structure assembly. A limited dispersal rate prohibits species reaching their preferred habitats, while a high dispersal rate leads to overdispersal such that species occur in unfavorable environments (Heino et al. 2015). Both of these scenarios can result in significant spatial signals. On the other hand, a significant environmental signal (i.e., species-sorting

mechanism) indicates that species get sorted to their favorable habitats (Leibold et al. 2004). The variation partitioning results show that environmental processes are significant but spatial processes are insignificant, suggesting that ostracode species composition is structured by species sorting coupled with a moderate dispersal rate (Ng et al. 2009). Shallow-marine ostracodes are generally poor dispersers that migrate by either "walking" or being carried by vectors such as ocean currents, ballast water, and flowing weed (Teeter 1973; Titterton and Whatley 1988). Passive migration due to fast-flowing (~26–34 cm/s) bottom-water current has been proposed as a controlling factor in recent distribution of warm, shallow-marine ostracode species in Japan (Tanaka 2008). The subsurface TWC, which can reach a maximum flow rate of ~30 cm/s (Zhu et al. 2004) may, therefore, potentially aid dispersal of ostracode species to favorable environments, while the rapid generation of shallow-marine ostracodes (Smith and Horne 2012) promotes their colonization.

Conclusions

Our results describe biotic responses to rapid environmental changes in the Changjiang delta. While ostracode species richness in the study area does not show systematic change relative to that of the 1980s, changes in relative abundance of key species showed characteristic patterns. These possibly resulted from anthropogenic activities such as urban development (i.e., eutrophication) and construction of dams (i.e., reduction of river water discharge). We have also demonstrated that environmental processes are more important than spatial processes for ostracode community structure in Changjiang estuary and its adjacent area. Integrating spatial variables generated by methods such as dbMEM into analysis not only improves our understanding of the mechanisms leading to the observed species distribution pattern, but also provokes consideration of context-dependent false-positive species–environment correlations represented by the explained variation of spatially structured environmental variables. Although this approach was recently applied on freshwater ostracode analyses (Escrivà et al. 2015; Zhai et al. 2015; Castillo-Escrivà et al. 2016), it has been underappreciated in marine ostracode studies. This study assesses ecological impacts of deteriorating Asian megadeltas and is especially significant for paleontological studies that derive past environmental conditions based on knowledge of modern species–environmental relationships.

Literature Cited

Abe, K. 1988. Speciation completed? In *Keijella bisanensis* species group. Developments in Palaeontology and Stratigraphy 11:919–925.

Athersuch, J., D. J. Horne, and J. E. Whittaker. 1989. Marine and brackish water ostracods. P. 343 *in* D. M. Kermaack and R. S. K. Barnes, eds. Synopses of the British fauna (New series). Brill, Leiden.

Baquero, O. S. 2017. ggsn: north symbols and scale bars for maps created with 'ggplot2' or 'ggmap', R package version 0.4.0. https://github.com/oswaldosantos/ggsn, accessed 26 February 2019.

Bianchi, T. S., and M. A. Allison. 2009. Large-river delta-front estuaries as natural "recorders" of global environmental change. Proceedings of the National Academy of Sciences USA 106:8085–8092.

Blanchet, F. G., P. Legendre, and D. Borcard. 2008. Forward selection of explanatory variables. Ecology 89:2623–2632.

Bodergat, A.-M., and N. Ikeya. 1988. Distribution of recent Ostracoda in Ise and Mikawa Bays, Pacific coast of central Japan. Developments in Palaeontology and Stratigraphy 11:413–428.

Boomer, I., and G. Eisenhauer. 2002. Ostracod faunas as palaeoenvironmental indicators in marginal marine environments. Pp. 135–149 *in* J. A. Holmes and A. R. Chivas, eds. The Ostracoda:

applications in Quaternary research. American Geophysical Union, Washington, DC.

Borcard, D., P. Legendre, and P. Drapeau. 1992. Partialling out the spatial component of ecological variation. Ecology 73:1045–1055.

Brouwers, E. M., T. M. Cronin, D. J. Horne, and A. R. Lord. 2000. Recent shallow marine ostracods from high latitudes: implications for late Pliocene and Quaternary palaeoclimatology. Boreas 29:127–142.

Buschke, F. T., L. De Meester, L. Brendonck, and B. Vanschoenwinkel. 2015. Partitioning the variation in African vertebrate distributions into environmental and spatial components—exploring the link between ecology and biogeography. Ecography 38:450–461.

Castillo-Escrivà, A., L. Valls, C. Rochera, A. Camacho, and F. Mesquita-Joanes. 2016. Spatial and environmental analysis of an ostracod metacommunity from endorheic lakes. Aquatic Sciences 78:707–716.

Chai, C., Z. Yu, Z. Shen, X. Song, X. Cao, and Y. Yao. 2009. Nutrient characteristics in the Yangtze River estuary and the adjacent East China Sea before and after impoundment of the Three Gorges Dam. Science of the Total Environment 407:4687–4695.

Chen, C., J. Zhu, R. C. Beardsley, and P. J. S. Franks. 2003. Physical-biological sources for dense algal blooms near the Changjiang River. Geophysical Research Letters 30(10). doi: 10.1029/2002GL016391.

Chen, C.-C., F.-K. Shiah, K.-P. Chiang, G.-C. Gong, and W. M. Kemp. 2009. Effects of the Changjiang (Yangtze) River discharge on planktonic community respiration in the East China Sea. Journal of Geophysical Research: Oceans 114(C3). doi: 10.1029/2008JC004891.

Chunlian, L., F. T. Fürsich, W. Jie, D. Yixin, Y. Tingting, Y. Jian, W. Yuan, and L. Min. 2013. Late Quaternary palaeoenvironmental changes documented by microfaunas and shell stable isotopes in the southern Pearl River delta plain, South China. Journal of Palaeogeography 2:344–361.

De Bie, T., L. De Meester, L. Brendonck, K. Martens, B. Goddeeris, D. Ercken, H. Hampel, L. Denys, L. Vanhecke, K. Van der Gucht, J. Van Wichelen, W. Vyverman, and S. A. J. Declerck. 2012. Body size and dispersal mode as key traits determining metacommunity structure of aquatic organisms. Ecology Letters 15:740–747.

De Master, D. J., B. A. McKee, C. A. Nittrouer, J. Qian and G. Cheng. 1985. Rates of sediment accumulation and particle reworking based on radiochemical measurements from continental shelf deposits in the East China Sea. Continental Shelf Research 4:143–158.

Dray, S., P. Legendre, and P. R. Peres-Neto. 2006. Spatial modelling: a comprehensive framework for principal coordinate analysis of neighbour matrices (PCNM). Ecological Modelling 196:483–493.

Dray, S., R. Pélissier, P. Couteron, M.-J. Fortin, P. Legendre, P. R. Peres-Neto, E. Bellier, R. Bivand, F. G. Blanchet, and M. De Cáceres. 2012. Community ecology in the age of multivariate multiscale spatial analysis. Ecological Monographs 82:257–275.

Dray, S., P. Legendre, and G. Blanchet. 2013. packfor: forward selection with permutation (Canoco p.46), R package version 0.0-8/r109. http://r-forge.r-project.org/projects/sedar, accessed 1 February 2019.

Dray, S., G. Blanchet, D. Borcard, G. Guenard, T. Jombart, G. Larocque, P. Legendre, N. Madi, and H. H. Wagner. 2017. adespatial: multivariate multiscale spatial analysis, R package version 0.0-8. https://cran.r-project.org/web/packages/adespatial/index.html, accessed 1 February 2019.

Duan, X., S. Liu, M. Huang, S. Qiu, Z. Li, K. Wang, and D. Chen. 2009. Changes in abundance of larvae of the four domestic Chinese carps in the middle reach of the Yangtze River, China, before and after closing of the Three Gorges Dam. Environmental Biology of Fishes 86:13.

Escrivà, A., J. M. Poquet, and F. Mesquita-Joanes. 2015. Effects of environmental and spatial variables on lotic ostracod metacommunity structure in the Iberian Peninsula. Inland Waters 5:283–294.

Frenzel, P., and I. Boomer. 2005. The use of ostracods from marginal marine, brackish waters as bioindicators of modern and Quaternary environmental change. Palaeogeography, Palaeoclimatology, Palaeoecology 225:68–92.

Fujiwara, O., F. Masuda, T. Sakai, T. Irizuki, and K. Fuse. 2000. Tsunami deposits in Holocene bay mud in southern Kanto region, Pacific coast of central Japan. Sedimentary Geology 135:219–230.

Gao, B., D. Yang, and H. Yang. 2013. Impact of the Three Gorges Dam on flow regime in the middle and lower Yangtze River. Quaternary International 304:43–50.

Gong, G.-C., J. Chang, K.-P. Chiang, T.-M. Hsiung, C.-C. Hung, S.-W. Duan, and L. A. Codispoti. 2006. Reduction of primary production and changing of nutrient ratio in the East China Sea: effect of the Three Gorges Dam? Geophysical Research Letters 33(7). doi: 10.1029/2006GL025800.

Gu, C., L. Hu, X. Zhang, X. Wang, and J. Guo. 2011. Climate change and urbanization in the Yangtze River delta. Habitat International 35:544–552.

Guo, H., Q. Hu, Q. Zhang, and S. Feng. 2012. Effects of the Three Gorges Dam on Yangtze River flow and river interaction with Poyang Lake, China: 2003–2008. Journal of Hydrology 416:19–27.

Heino, J., A. S. Melo, T. Siqueira, J. Soininen, S. Valanko, and L. M. Bini. 2015. Metacommunity organisation, spatial extent and dispersal in aquatic systems: patterns, processes and prospects. Freshwater Biology 60:845–869.

Hong, Y., M. Yasuhara, H. Iwatani, and B. Mamo. 2019. Baseline for ostracod-based northwestern Pacific and Indo-Pacific shallow-marine paleoenvironmental reconstructions: ecological modeling of species distributions. Biogeosciences 16:585-604.

Hou, Y., and Y. Gou. 2007. Fossil Ostracoda of China. Volume 2: Cytheracea and Cytherellidae. Science Publishing House, Beijing.

Hsieh, T. C., K. H. Ma, and A. Chao. (2016), iNEXT: an R package for rarefaction and extrapolation of species diversity (Hill numbers). Methods in Ecology and Evolution 7:1451–1456.

Irizuki, T., H. Takata, and K. Ishida. 2006. Recent Ostracoda from Urauchi Bay, Kamikoshiki-jima Island, Kagoshima Prefecture, southwestern Japan. Laguna 13:13–28.

Irizuki, T., A. Takimoto, M. Sako, R. Nomura, K. Kakuno, A. Wanishi, and S. Kawano. 2011. The influences of various anthropogenic sources of deterioration on meiobenthos (Ostracoda) over the last 100 years in Suo-Nada in the Seto Inland Sea, southwest Japan. Marine Pollution Bulletin 62:2030–2041.

Irizuki, T., H. Ito, M. Sako, K. Yoshioka, S. Kawano, R. Nomura, and Y. Tanaka. 2015. Anthropogenic impacts on meiobenthic Ostracoda (Crustacea) in the moderately polluted Kasado Bay, Seto Inland Sea, Japan, over the past 70 years. Marine Pollution Bulletin 91:149–159.

Jiao, N., Y. Zhang, Y. Zeng, W. D. Gardner, A. V. Mishonov, M. J. Richardson, N. Hong, D. Pan, X.-H. Yan, Y.-H. Jo, C.-T. A. Chen, P. Wang, Y. Chen, H. Hong, Y. Bai, X. Chen, B. Huang, H. Deng, Y. Shi, and D. Yang. 2007. Ecological anomalies in the East China Sea: impacts of the Three Gorges Dam? Water Research 41:1287–1293.

Kahle, D., and H. Wickham. 2013. ggmap: spatial visualization with ggplot2. The R Journal 5:144–161.

Kako, S. i., T. Nakagawa, K. Takayama, N. Hirose, and A. Isobe. 2016. Impact of Changjiang River Discharge on sea surface temperature in the East China Sea. Journal of Physical Oceanography 46:1735–1750.

Kelley, L. A., S. P. Gardner, and M. J. Sutcliffe. 1996. An automated approach for clustering an ensemble of NMR-derived protein structures into conformationally related subfamilies. Protein Engineering, Design and Selection 9:1063–1065.

Legendre, P., and E. D. Gallagher. 2001. Ecologically meaningful transformations for ordination of species data. Oecologia 129:271–280.

Legendre, P., and L. F. Legendre. 2012. Numerical ecology, 3rd English ed. Elsevier Science, Amsterdam.

Leibold, M. A., M. Holyoak, N. Mouquet, P. Amarasekare, J. M. Chase, M. F. Hoopes, R. D. Holt, J. B. Shurin, R. Law, and D. Tilman. 2004. The metacommunity concept: a framework for multi-scale community ecology. Ecology Letters 7:601–613.

Lie, H.-J., C.-H. Cho, J.-H. Lee, and S. Lee. 2003. Structure and eastward extension of the Changjiang River plume in the East China Sea. Journal of Geophysical Research: Oceans 108(C3). doi: 10.1029/2001JC001194

Liu, J. P., A. C. Li, K. H. Xu, D. M. Velozzi, Z. S. Yang, J. D. Milliman, and D. J. DeMaster. 2006. Sedimentary features of the Yangtze River-derived along-shelf clinoform deposit in the East China Sea. Continental Shelf Research 26:2141–2156.

Locarnini, R. A., A. V. Mishonov, J. I. Antonov, T. P. Boyer, H. E. Garcia, O. K. Baranova, M. M. Zweng, C. R. Paver, J. R. Reagan, D. R. Johnson, M. Hamilton, and D. Seidov. 2013. World ocean atlas 2013, Vol. 1. Temperature. In S. Levitus, ed.; A. Mishonov, technical ed. NOAA atlas NESDIS 73. National Oceanographic Data Center, Silver Spring, Md.

McKee, B. A., R. C. Aller, M. A. Allison, T. S. Bianchi, and G. C. Kineke. 2004. Transport and transformation of dissolved and particulate materials on continental margins influenced by major rivers: benthic boundary layer and seabed processes. Continental Shelf Research 24:899–926.

Meybeck, M., H. H. Dürr, and C. J. Vörösmarty. 2006. Global coastal segmentation and its river catchment contributors: a new look at land–ocean linkage. Global Biogeochemical Cycles 20(1). doi: 10.1029/2005GB002540.

Meybeck, M., and C. Vörösmarty. 2005. Fluvial filtering of land-to-ocean fluxes: from natural Holocene variations to Anthropocene. Comptes Rendus Geoscience 337:107–123.

NASA Goddard Space Flight Center, Ocean Ecology Laboratory, and Ocean Biology Processing Group. 2014. Moderate-resolution imaging spectroradiometer (MODIS) aqua chlorophyll data, 2014 reprocessing. NASA OB.DAAC, Greenbelt, Md. doi: 10.5067/AQUA/MODIS/L3M/CHL/2014.

Ng, I. S., C. M. Carr, and K. Cottenie. 2009. Hierarchical zooplankton metacommunities: distinguishing between high and limiting dispersal mechanisms. Hydrobiologia 619:133–143.

Nilsson, C., C. A. Reidy, M. Dynesius, and C. Revenga. 2005. Fragmentation and flow regulation of the world's large river systems. Science 308:405–408.

O'Brien, R. M. 2007. A caution regarding rules of thumb for variance inflation factors. Quality and Quantity 41:673–690.

Oksanen, J., F. G. Blanchet, M. Friendly, R. Kindt, P. Legendre, D. McGlinn, P. R. Minchin, R. B. O'Hara, G. L. Simpson, P. Solymos, M. H. H. Stevens, E. Szoecs, and H. Wagner. 2017. vegan: community ecology package, R package version 2.4-3. https://cran.r-project.org/src/contrib/Archive/vegan, accessed 1 February 2019.

Ozawa, H., T. Kamiya, H. Itoh, and S. Tsukawaki. 2004. Water temperature, salinity ranges and ecological significance of the three families of recent cold-water ostracods in and around the Japan Sea. Paleontological Research 8:11–28.

Pei, S., Z. Shen, and E. A. Laws. 2009. Nutrient dynamics in the upwelling area of Changjiang (Yangtze River) estuary. Journal of Coastal Research 25:569–580.

Peres-Neto, P. R., P. Legendre, S. Dray, and D. Borcard. 2006. Variation partitioning of species data matrices: estimation and comparison of fractions. Ecology 87:2614–2625.

Peres-Neto, P. R., and P. Legendre. 2010. Estimating and controlling for spatial structure in the study of ecological communities. Global Ecology and Biogeography 19:174–184.

R Core Team. 2017. R: a language and environment for statistical computing. R Foundation for Statistical Computing, Vienna, Austria.

Saito, Y., N. Chaimanee, T. Jarupongsakul, and J. P. Syvitski. 2007. Shrinking megadeltas in Asia: sea-level rise and sediment reduction impacts from case study of the Chao Phraya delta. Inprint Newsletter of the IGBP/IHDP Land Ocean Interaction in the Coastal Zone 2007(2):3–9.

Schellenberg, S. 2007. Marine ostracods. Pp. 2046–2062 in S. Elias, ed. Encyclopedia of Quaternary science. Elsevier, Amsterdam.

Shao, M.-L., Z.-C. Xie, X.-Q. Han, M. Cao, and Q.-H. Cai. 2008. Macroinvertebrate community structure in Three-Gorges Reservoir, China. International Review of Hydrobiology 93:175–187.

Smith, A. J., and D. J. Horne. 2012. Ecology of marine, marginal marine and nonmarine Ostracodes. Pp. 37–64 in J. A. Holmes and A. R. Chivas, eds. The Ostracoda: applications in Quaternary research. American Geophysical Union, Washington, DC.

Su, C. C., and C. A. Huh. 2002. ^{210}Pb, ^{137}Cs and ^{239,240}Pu in East china Sea sediments: sources, pathways and budgets of sediments and radionuclides. Marine Geology 183:163–178.

Syvitski, J. P. M., A. J. Kettner, I. Overeem, E. W. H. Hutton, M. T. Hannon, G. R. Brakenridge, J. Day, C. Vorosmarty, Y. Saito, L. Giosan, and R. J. Nicholls. 2009. Sinking deltas due to human activities. Nature Geoscience 2:681–686.

Tanaka, G. 2008. Recent benthonic ostracod assemblages as indicators of the Tsushima Warm Current in the southwestern Sea of Japan. Hydrobiologia 598:271–284.

Teeter, J. W. 1973. Geographic distribution and dispersal of some Recent shallow-water marine Ostracoda. Ohio Journal of Science 73:46–54.

Titterton, R., and R. C. Whatley. 1988. The provincial distribution of shallow water Indo-Pacific marine Ostracoda: origins, antiquity, dispersal routes and mechanisms. Developments in Palaeontology and Stratigraphy 11:759–786.

Tsai, A.-Y., G.-C. Gong, R. W. Sanders, C.-J. Wang, and K.-P. Chiang. 2010. The impact of the Changjiang River plume extension on the nanoflagellate community in the East China Sea. Estuarine, Coastal and Shelf Science 89:21–30.

Wang, H., Y. Saito, Y. Zhang, N. Bi, X. Sun, and Z. Yang. 2011. Recent changes of sediment flux to the western Pacific Ocean from major rivers in East and Southeast Asia. Earth-Science Reviews 108:80–100.

Wang, J., J. Huang, J. Wu, X. Han, and G. Lin. 2010. Ecological consequences of the Three Gorges Dam: insularization affects foraging behavior and dynamics of rodent populations. Frontiers in Ecology and the Environment 8:13–19.

Wang, J., W. Yan, N. Chen, X. Li, and L. Liu. 2015. Modeled long-term changes of DIN:DIP ratio in the Changjiang River in relation to Chl-α and DO concentrations in adjacent estuary. Estuarine, Coastal and Shelf Science 166:153–160.

Wang, P., and Q. Zhao. 1985. Ostracod distribution in bottom sediments of the East China Sea. Pp. 70–92 in P. Wang, ed. Marine micropaleontology of China. China Ocean Press, Beijing. [In Chinese.]

Wang, P., P. Zhang, Q. Zhao, Q. Min, Y. Bian, L. Zheng, X. Cheng, and R. Chen. 1988. Foraminifera and Ostracoda in bottom sediments of the East China Sea. China Ocean Press, Beijing.

White, D., and R. Gramacy. 2012. maptree: mapping, pruning, and graphing tree models, R package version 1.4–7. https://cran.r-project.org/web/packages/maptree/index.html, accessed 1 February 2019.

Wickham, H. 2016. ggplot2: elegant graphics for data analysis. Springer-Verlag New York.

Woodroffe, C. D., and Y. Saito. 2011. River-dominated coasts. In: E. Wolanski and D. S. McLusky, eds. Treatise on estuarine and coastal science 3:117–135. Waltham: Academic.

Wu, J., J. Huang, X. Han, X. Gao, F. He, M. Jiang, Z. Jiang, R. B. Primack, and Z. Shen. 2004. The Three Gorges Dam: an ecological perspective. Frontiers in Ecology and the Environment 2:241–248.

Yang, H., S. Yang, K. Xu, J. Milliman, H. Wang, Z. Yang, Z. Chen, and C. Zhang. 2018. Human impacts on sediment in the Yangtze River: a review and new perspectives. Global and Planetary Change 162:8–17.

Yang, S. L., K. H. Xu, J. D. Milliman, H. F. Yang, and C. S. Wu. 2015. Decline of Yangtze River water and sediment discharge: impact from natural and anthropogenic changes. Scientific Reports 5:12581.

Yasuhara, M., S. Yoshikawa, and F. Nanayama. 2005. Reconstruction of the Holocene seismic history of a seabed fault using relative sea-level curves reconstructed by ostracode assemblages: case study on the Median Tectonic Line in Iyo-nada Bay, western Japan. Palaeogeography, Palaeoclimatology, Palaeoecology 222:285–312.

Yasuhara, M., and K. Seto. 2006. Holocene relative sea-level change in Hiroshima Bay, Japan: a semi-quantitative reconstruction based on ostracodes. Paleontological Research 10:99–116.

Yasuhara, M., H. Yamazaki, A. Tsujimoto, and K. Hirose. 2007. The effect of long-term spatiotemporal variations in urbanization-induced eutrophication on a benthic ecosystem, Osaka Bay, Japan. Limnology and Oceanography 52:1633–1644.

Yasuhara, M., G. Hunt, D. Breitburg, A. Tsujimoto, and K. Katsuki. 2012a. Human-induced marine ecological degradation: micropaleontological perspectives. Ecology and Evolution 2:3242–3268.

Yasuhara, M., G. Hunt, G. van Dijken, K. R. Arrigo, T. M. Cronin, and J. E. Wollenburg. 2012b. Patterns and controlling factors of species diversity in the Arctic Ocean. Journal of Biogeography 39:2081–2088.

Yasuhara, M., D. P. Tittensor, H. Hillebrand, and B. Worm. 2017. Combining marine macroecology and palaeoecology in understanding biodiversity: microfossils as a model. Biological Reviews 92:199–215.

Zhai, M., O. Nováček, D. Výravský, V. Syrovátka, J. Bojková, and J. Helešic. 2015. Environmental and spatial control of ostracod assemblages in the Western Carpathian spring fens. Hydrobiologia 745:225–239.

Zhao, Q. 1987. A study of the distribution of Recent ostracod faunas from the coastal areas of the East China and Yellow Seas. Acta Oceanographica Sinica 6:413–420.

Zhao, Q., and P. Wang. 1988. Distribution of modern Ostracoda in the shelf seas off China. Developments in Palaeontology and Stratigraphy 11:805–821.

Zhu, J., C. Chen, P. Ding, C. Li, and H. Lin. 2004. Does the Taiwan warm current exist in winter? Geophysical Research Letters 31 (12). doi: 10.1029/2004GL019997.

Zweng, M. M., J. R. Reagan, J. I. Antonov, R. A. Locarnini, A. V. Mishonov, T. P. Boyer, H. E. Garcia, O. K. Baranova, D. R. Johnson, D. Seidov, and M. M. Biddle. 2013. World ocean atlas 2013, Vol. 2. Salinity. In S. Levitus, ed.; A. Mishonov, technical ed. NOAA atlas NESDIS 74. National Oceanographic Data Center, Silver Spring, Md.